International Journal of Heat and Mass Transfer 52 (2009) 4873–4882

Contents lists available at ScienceDirect

International Journal of Heat and Mass Transfer

journal homepage: www.elsevier.com/locate/ijhmt

A physical picture of the mechanism of turbulent heat transfer from the wall

Phuong M. Le, Dimitrios V. Papavassiliou *

School of Chemical, Biological and Materials Engineering, The University of Oklahoma, 100 East Boyd, Norman, OK 73019, USA

ARTICLE INFO

Article history:
Received 2 September 2008
Received in revised form 2 May 2009
Accepted 2 May 2009

Keywords:
Turbulent transport
Lagrangian methods
Turbulent Prandtl number

ABSTRACT

The present work investigates the correlation between the velocity and the temperature field in wall turbulence using direct numerical simulation of turbulent channel flow and plane Couette flow in conjunction with a Lagrangian method. Characteristic length scales for heat transfer are calculated for fluids with Prandtl numbers between 0.1 and 100. Structures of larger scales are found to contribute to the transport of heat as the distance from the wall increases. Turbulent Prandtl numbers are then calculated, showing that the turbulent Prandtl number is a function of the distance from the wall, but it does not depend on the fluid Prandtl number for high Prandtl numbers.

1. Introduction

Turbulent channel flows have been investigated using numerical methods and results have been reported by several researchers during the last two decades due to the fast development of high end computing systems. In the review by Robinson [1], coherent motions, or the narrow streaks of velocity in the viscous sublayer and buffer region, were found to be responsible for the maintenance of turbulence in turbulent boundary layers. Recently, these coherent motions and hairpin vortex structures were possible to study at higher Reynolds number [2–12]. The significance of turbulence structure in the near-wall region in turbulent heat transport away from the wall has been explored both experimentally and numerically. Results indicate that large-scale motions may dominate turbulent transport in all regions except the very near-wall layer [9]. However, the mechanism of passive heat transfer away from the wall has still not been explored and interpreted clearly.

There is some speculation about the correlation between the velocity structure and the temperature field [2,3,6]. Kawamura et al. investigated how the turbulent flow affects heat transfer [13,14]. The instantaneous flow and thermal fields were visualized using direct numerical simulations in order to investigate the structure of streaks and vortices for low Prandtl number, *Pr*, fluids in turbulent channel flow. It was found that large-scale structures affect the surface heat-flux fluctuations and that the surface heat-flux fluctuations are similar to the streamwise wall shear-stress fluctuations, while a noticeable dissimilarity was observed for large positive or negative fluctuations. Kasagi and Ohtsubo [15] presented low and high temperature regions, as well as the fluctuating velocity vectors that are associated with these regions. They showed that there was some correlation between the velocity field and the thermal field. The magnitude of the velocity fluctuations was higher at low temperature regions. Furthermore, the contours of the magnitude of these vectors were related to the shape and size of the thermal regions. These prior investigations have found that the velocity and the temperature streaks show a strong resemblance to each other, but they do not describe how the heat can be carried by the vortices into the flow.

The contribution of the present work is to provide a physical picture of the kinematics of the mechanism of heat transfer from the wall and to investigate the importance of the velocity structure at the wall by using a Lagrangian method (Lagrangian scalar tracking, LST) coupled with a direct numerical simulation (DNS) of turbulent channel and plane Couette flow for a range of Prandtl numbers. The velocity structure and the thermal field for fluids with Prandtl number, *Pr*, between 0.1 and 100, as well as the case of dispersion of simple fluid particles, were studied and visualized to explore the correlation between them. Particles representing heat markers that are released from a single line source located at the channel wall were also tracked and studied downstream from the point of release, in order to investigate how eddies can carry these heat markers away from the wall.

Turbulent transport results using the DNS/LST method published previously from our research group in plane channel flow [16–19] and in plane Couette flow [20,21] for a range of *Pr* from 0.1 to 50,000 have shown agreement with data obtained with Eulerian methods in other laboratories. In this present work, the characteristic length scales for momentum transfer and for scalar transfer are calculated for different Prandtl number fluids across

* Corresponding author. Address: School of Chemical, Biological and Materials Engineering, The University of Oklahoma, 100 East Boyd Street, SEC T-335, Norman, OK 73019, USA. Tel.: +1 405 3255811; fax: +1 405 3255813.
E-mail address: dvpapava@ou.edu (D.V. Papavassiliou).

0017-9310/$ - see front matter © 2009 Elsevier Ltd. All rights reserved.
doi:10.1016/j.ijheatmasstransfer.2009.05.024

Nomenclature

C	scalar profile
c'	fluctuation
C_p	specific heat at constant pressure
E_v	eddy viscosity
E_α	eddy diffusivity
h	half-height of the channel in viscous wall units
L_M	length scale characterizing the motion of fluid particles
L_T	length scale characterizing the motion of heat markers, defined in Eq. (9)
l_M	mixing length of momentum in viscous wall units
l_T	scalar mixing length in viscous wall units
N_y, N_z	numbers of bins in the y and z directions
P_1	conditional probability for a marker to be at a location (x, y, z) at time t, given that it was released at a known time from a known location
P_2	joint probability for a marker to be at a location (y, z)
Pr	Prandtl number, $Pr = \nu/\alpha$
Pr_τ	turbulent Prandtl number, $Pr_\tau = E_v/E_\alpha$
q_w	heat flux from the wall
Re	Reynolds number, $Re = U_c h/\nu$
R_{TT}	two-point correlation coefficient
T	temperature
T^*	friction temperature, $T^* = q_w/(\rho C_p u^*)$
$\overline{\theta v'}$	turbulent heat flux in the normal direction
t	time in viscous wall units
t_o, t_f	initial and final time of tracking markers in viscous wall units
t_1	time at which more than 2000 heat markers are captured at $140 < x - x_o < 160$
U	velocity
U_c	centerline mean velocity
u^*	friction velocity, $u^* = (\tau_w/\rho)^{1/2}$
$\overline{u'v'}$	Reynolds stress
u', v'	velocity fluctuations in the streamwise and normal directions
$\vec{V}$	Lagrangian velocity vector
x, y, z	streamwise, normal and spanwise coordinates
x_f	final streamwise position of tracking markers

Greek symbols

α	thermal diffusivity
δ	average thickness of heat marker clouds that transfer heat from the wall
Δt	time step
θ	temperature fluctuation
ν	kinematic viscosity
π	trigonometric pi ($\pi = 3.14159\ldots$)
ρ	fluid density
σ	standard deviation of a probability density function
τ	shear stress

Superscripts and subscripts

$\overline{()}$	average value
$\vec{()}$	vector quantity
$()^*$	friction value
$()_o$	value at the instant of marker release
$()_w$	value at the wall of the channel

the channel. Similarly to the model of Crimaldi et al. [22], the turbulent Prandtl number can be calculated by finding the ratio of the turbulent length scales.

2. Length scales and turbulent Prandtl number – background

The turbulent Prandtl number, Pr_τ, is a measure of the relative rate of mixing of momentum and a scalar quantity at a given location in the flow. It plays a crucial role in modeling turbulent transport. Quoting from Churchill [23]: "the development of a comprehensive predictive or correlative expression for the turbulent Prandtl number is the principal remaining challenge with respect to the prediction of turbulent forced convection." However, the turbulent Prandtl number is still calculated approximately, and available models for its prediction vary a great deal. The simplest model for Pr_τ is the Reynolds analogy [24], which yields a Pr_τ of 1. Reported experimental data indicate that the value of Pr_τ is 0.85 [25,26], but ranging from 0.7 to 0.9 depending on the fluid in question. The most often used model is Kay's model [27]. Churchill and Chan [28] modified Kay's formula based on turbulence scaling that is defined by the fraction of heat flux due to turbulence, instead of the conventional viscous scaling.

Crimaldi et al. [22] proposed a model based on simple knowledge of the geometric and kinematic nature of the momentum and scalar boundary conditions. They utilized the concept of a hypothetical "mixing length" proposed by Prandtl. This model relates the Reynolds stress to the mean velocity gradient through the relationship

$$\overline{u'v'} = -l_M^2 \left|\frac{\partial \overline{U}}{\partial y}\right| \frac{\partial \overline{U}}{\partial y} \tag{1}$$

where l_M is an assumed mixing length of momentum. They modeled the behavior of the vertical scalar flux $\overline{\theta v'}$ in terms of a scalar mixing length as follows:

$$\overline{\theta v'} = -l_M \frac{\partial \overline{U}}{\partial y} l_T \frac{\partial \overline{T}}{\partial y} \tag{2}$$

where l_T is the scalar mixing length. The turbulent Prandtl number was then calculated as

$$Pr_\tau \equiv \frac{E_v}{E_\alpha} = \frac{\overline{u'v'}/(\partial \overline{U}/\partial y)}{\overline{\theta v'}/(\partial \overline{T}/\partial y)} = \frac{l_M}{l_T} \tag{3}$$

3. Methodology

3.1. Lagrangian scalar tracking

The study of heat and mass transfer using the DNS/LST methodology can be found in several prior publications [16–21,29–31]. The basic concept of Lagrangian scalar tracking (LST) is that passive scalar transport in turbulent flow is the result of the combined behavior of an infinite number of continuous sources of heat or mass markers. For the present study, the trajectories of heat markers in the flow field created by a DNS were calculated using the tracking algorithm of Kontomaris et al. [32]. The marker motion was decomposed into a convective part and a molecular diffusion part. The convective part was calculated from the fluid velocity at the marker position yielding for the equation of particle motion $\vec{V}(\vec{x}_o, t) = \frac{\partial \vec{x}(\vec{x}_o, t)}{\partial t}$, where the Lagrangian velocity of a marker released at location $\vec{x}_o$ is given as $\vec{V}(\vec{x}_o, t) = \vec{U}[\vec{x}(\vec{x_o}, t), t]$ ($\vec{U}$ is the Eulerian velocity of the fluid at the location of the marker at time t). The effect of molecular diffusion was calculated following Einstein's

theory for Brownian motion; the diffusion effect was simulated by adding a 3D random walk on the particle motion at the end of every convection step. The size of the random jump in each one of the three space directions took values from a Gaussian distribution with zero mean and a standard deviation of $\sigma = \sqrt{2\Delta t/Pr}$ in viscous wall units. (It is customary in wall turbulence to make quantities dimensionless using the friction velocity, u^*, and friction temperature, T^*, at the wall. Quantities made dimensionless in this manner are defined as "wall" or "viscous" quantities. All quantities in this work are expressed in viscous wall units unless otherwise specified.) Effects of Pr on the process can thus be studied by modifying σ. This allows the LST methodology to simulate fluids within an extensive range of Pr.

3.2. Direct numerical simulations

DNS has proven to be a successful and useful methodology to study heat transfer in turbulent flows [14,33–37]. In the present work, the flow was for an incompressible Newtonian fluid with constant physical properties. In the case of channel flow, the flow was driven by a constant mean pressure gradient, and for the case of plane Couette flow it was driven by the shear of the walls of the channel that move in opposite directions. The Reynolds number, defined with the centerline mean velocity and the half-height of the channel for the Poiseuille flow channel, and defined with half the velocity difference between the two walls and the half channel height for the Couette flow channel, was 2660 for both. For the Poiseuille channel, the simulation was conducted on a $128 \times 65 \times 128$ grid in x, y, z, and the dimensions of the computational box were $4\pi h \times 2h \times 2\pi h$, where $h = 150$ in viscous wall units. For the Couette flow channel, the simulation was conducted on a $256 \times 65 \times 128$ grid, and the dimensions of the computational box were $8\pi h \times 2h \times 2\pi h$, where $h = 153$. The flow was regarded as periodic in the x and z directions, with the periodicity lengths equal to the dimensions of the computational box in these directions. The DNS used here is based on the pseudospectral algorithm by Lyons et al. [34] that has been validated previously [34,38,39]. The time step for the calculations of the hydrodynamic field and the Lagrangian tracking was $\Delta t = 0.25$ and $\Delta t = 0.2$ for the Poiseuille and Couette flow channels, respectively.

The behavior of a scalar line source was determined by following the paths of many scalar markers in the flow field created by the DNS. Both the channel and Couette flow simulations were first allowed to reach a stationary state before the heat markers were released. The simulated cases were for $Pr = 0.1$, 0.7, 6, 10, 100 and for the case of fluid particles, i.e., markers that do not exhibit the Brownian motion at the end of each time step. In plane Poiseuille flow, 16,129 particles were released for every simulation run. In plane Couette flow, where the computational domain is longer, 145,161 particles were released instantaneously at $y_o = 0$. In the case of fluid particles, the point of release was two viscous wall units away from the wall ($y_o = 2$), since particles without Brownian motion (and, thus, without a jump in the y direction) cannot escape the wall, where the fluid velocity is zero in all directions. The simulations were allowed to run up to the time when the average of the normal positions of the cloud is 75, which is equal to $h/2$, because we wanted to focus on the transfer of heat from the wall. The final simulation time for $Pr = 0.1$, 0.7, 6, 10 is 500 and for $Pr = 100$ is 1000. Six different runs were conducted for each type of flow and for each Pr, in order to obtain meaningful statistics for the calculated quantities. Each one of these six runs was initiated with a different initial velocity field at stationary state, and each of the initial velocity fields was taken at different times, so that the time difference between them was longer than the Eulerian integral time scale.

4. Results and discussion

4.1. Mechanism of heat transfer away from the wall

The behavior of an instantaneous line source of markers located at the wall of the channel can be described by the probability density function $P_1(\vec{x}, t|\vec{x_o}, t_o)$, of a marker to be at a location = (x, y, z) in the flow field at time t, given that it was released at location $\vec{x}_o = (x_o, y_o, z_o)$ at time t_o. This probability can be interpreted physically as temperature or as concentration [30,40], and thus as a snapshot of a cloud of contaminants released instantaneously from $\vec{x}_o$.

The behavior of a continuous line source located at x_o that emits markers from time t_o to time t_f can be calculated by integrating (or, in the discrete case, summing up) the probability density function P_1 as follows:

$$P_2(x, y, z, t_f|x_o, t_o) = \sum_{t=t_o}^{t_f} P_1(\vec{x}, t|\vec{x_o}, t_o) \tag{4}$$

where t_f is the final time of integration. This probability function P_2 represents the temperature profile downstream from the source. An average temperature was then calculated as a function of normal position by averaging P_2 in the streamwise direction, representing the temperature profile (or in the case of mass transfer the concentration profile) projected in the y–z plane, as follows:

$$C(y, z) = \sum_{x=x_o}^{x_f} P_2(x, y, z, t_f|x_o, t_o) \tag{5}$$

Since our simulation followed a finite number of heat markers, the y–z cross-section of the channel was divided into uniform, rectangular bins with $N_y = 300$ bins in the y direction and $N_z = 100$ bins in the z direction. An average temperature was then calculated as a function of normal position by averaging C in the spanwise direction

$$\overline{C}(y) = \frac{1}{N_z} \sum_{i=1}^{N_z} C(y, z_i) \tag{6}$$

where z_i is the z location of the center of bin i. A fluctuation, defined as C at a (y, z) point minus the z-averaged value of C at that normal location, marks a hot streak if the fluctuation is positive, and it marks the location of a cold streak if the fluctuation has a negative value. The locations of these hot and cold streaks can be found by calculating this fluctuation as

$$c'(y, z) = C(y, z) - \overline{C}(y) \tag{7}$$

Since C is an average over the x direction, contours of c' calculated from Eq. (7) show that the particles are distributed uniformly across the channel (i.e., in the y–z plane) as time progresses. The fluctuation contour plots for both plane channel and plane Couette flow do not show any structure of hot or cold regions.

The same analysis was repeated for a subset of the heat markers. This subset included only markers that have positive velocity in the vertical direction ($v' > 0$), i.e., only the markers that are moving away from the bottom wall. These are the markers that transfer heat away from the wall region, and contribute to the generation of turbulent heat flux. The same analysis was also done for the subset of markers that are moving towards the bottom wall ($v' < 0$). The fluctuation contour plots for the markers with $v' > 0$ are shown in Fig. 1(a) and (b) for $Pr = 0.7$ and $Pr = 100$, respectively. As expected, particles move faster into the flow field for lower Pr due to higher molecular diffusivity. Both figures show an overall resemblance to the case with fluid particles released at $y_o = 2$, shown in Fig. 1(c). This agrees with findings by Kawamura et al. [13,14] and Kasagi

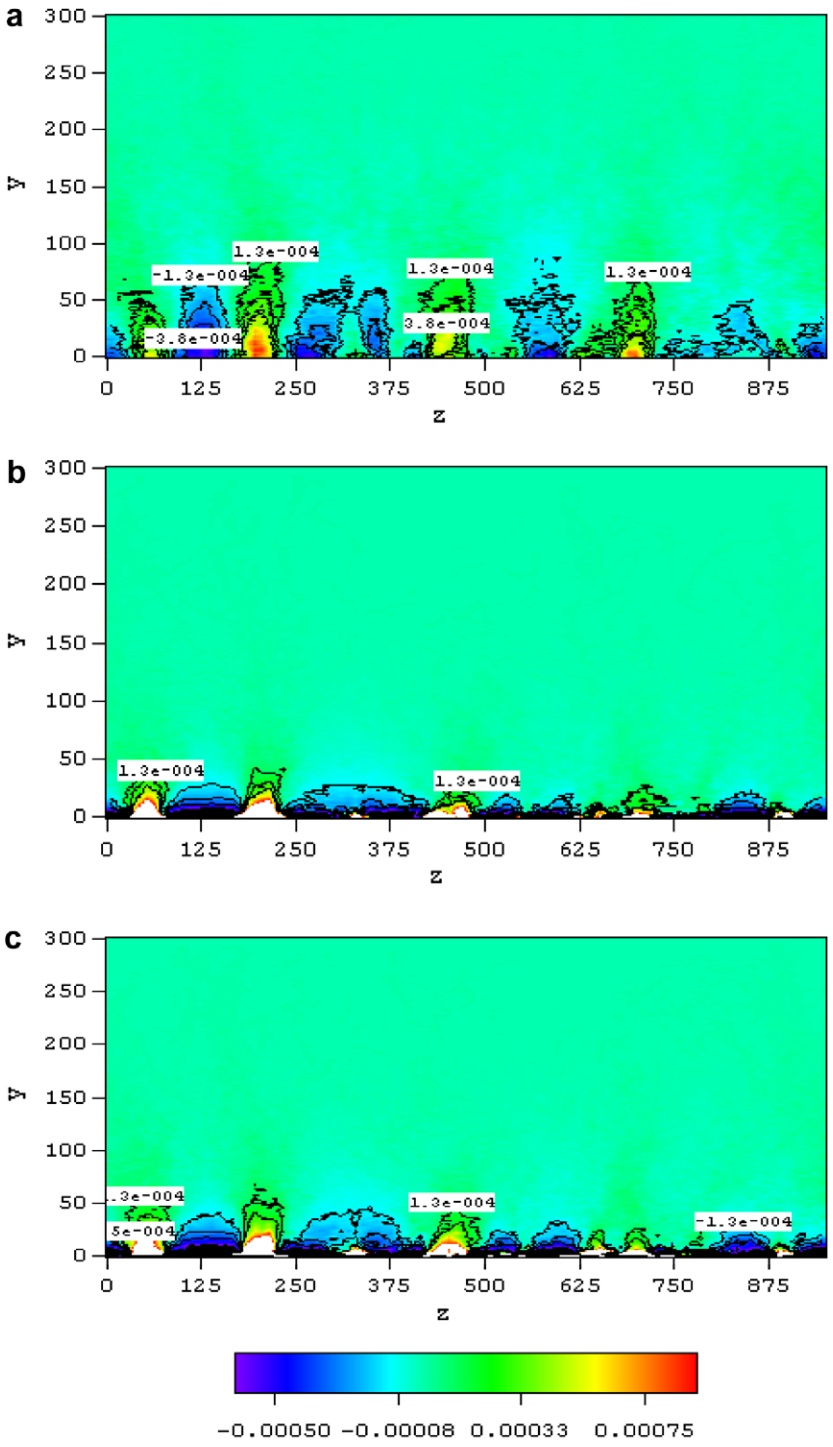

Fig. 1. Contour plot of the fluctuations of the heat marker concentration given that the markers are moving away from the wall ($v' > 0$) in plane channel flow at $t = 500$ for: (a) $Pr = 0.7$, (b) $Pr = 100$, (c) fluid particles.

et al. [33] that thermal streaks exist and that momentum streaks are related to the thermal streaks.

In order to further explore the momentum-heat correlation, transport in a different velocity field (Couette flow) was simulated. In plane Couette flow, the contour plots of fluctuations of particle concentration that are moving away from the wall also show the resemblance between the thermal field and the velocity structure. The contour plots of temperature fluctuations for markers moving away from the wall are shown in Fig. 2 for (a) $Pr = 0.7$, (b) $Pr = 100$, and (c) fluid particles. Plane Couette flow exhibits a different velocity structure from plane channel flow, due to the different mechanism that generates the flow. In plane channel flow, many small eddies are present at the wall. In plane Couette flow, it is common to observe large, streamwise-oriented vortical structures that extend longer than eddies in Poiseuille channel flow. As a result, the thermal field also shows structures that extend through the height of the channel. Similar observations were done for the case of markers with $v' < 0$ (not shown here).

The picture that emerges from Figs. 1 and 2, i.e., that velocity eddies contribute to the transfer of heat from the wall acting as

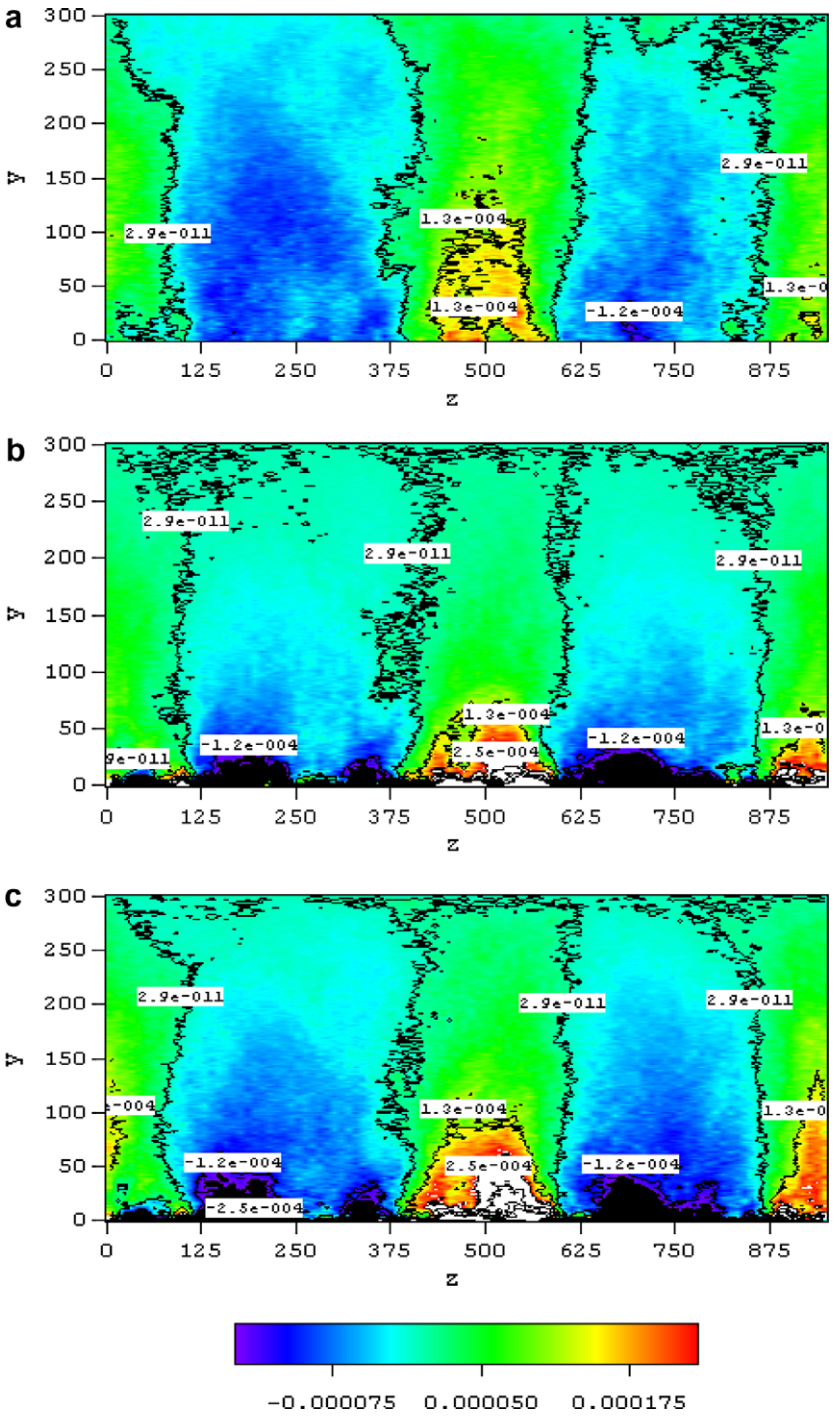

Fig. 2. Contour plot of the fluctuations of the heat marker concentration given that the markers are moving towards from the wall ($v' > 0$) in plane Couette flow at $t = 500$ for: (a) $Pr = 0.7$, (b) $Pr = 100$, (c) fluid particles.

"pumps" of heat, needs to be further investigated. How do individual eddies transfer heat, and is the whole eddy structure contributing to transfer or only the perimeter of the eddies? Do all eddies contribute equally? In order to elucidate the mechanism of heat transfer away from the wall, 100,000 particles were released from a single instantaneous line source located on the Poiseuille channel wall. The runs were repeated using different velocity fields to obtain better statistics for each Pr case. The velocities and trajectories of the particles were stored. We then focused at a distance downstream of the instantaneous source equal to the channel half-height. This is a distance at which, on average, the heat markers move out of the thermal sublayer and enter the log-layer [17]. Therefore, we captured the velocities and locations of particles that are moving through the thin interval $140 \leqslant x - x_o \leqslant 160$ (this is equivalent to observing a swarm of markers that are passing by a stationary window of observation as time elapses). The time t_1, at which the line source behavior for each Pr is studied, is different. It is the time at which at least 2000 markers were captured moving through the window $140 \leqslant x - x_o \leqslant 160$. As Pr increases, the heat markers have smaller molecular diffusion, they move towards the outer flow region slower, and therefore, they have on average smaller streamwise velocity and it takes longer for the heat mark-

ers to move to the same streamwise distance. Times of capture and numbers of markers captured are presented in Table 1.

The locations of the particles moving away from the bottom wall are shown in Fig. 3(a) and the locations of the particles moving toward the bottom wall at the downstream location $140 \leqslant x - x_o \leqslant 160$ are shown in Fig. 3(b). There are approximately 6% of the total number of markers present for $Pr = 0.7$. The corresponding figures for $Pr = 100$ are Fig. 4(a and b). The markers that are moving away from the bottom wall mark the location of $\overline{\theta v'} > 0$ events, since they indicate heat transferred from the hot wall by $v' > 0$ fluctuations. These quadrant one events (in the θ–v' space) are producers of turbulent heat flux. Similarly, particles that are moving towards the bottom wall mark the location of quadrant three events in the θ–v' space, since they indicate heat transferred to the wall from the center of the channel by $v' < 0$ fluctuations. These events are also producers of turbulent heat flux. As the Pr increases, the thickness of individual clouds of markers indicating quadrant one events decreases, indicating that a different part of a velocity eddy contributes to turbulent heat transfer for different Pr fluids.

The average thickness of the clouds of markers was calculated and presented in Fig. 5 for different distances from the wall ($y = 2$, 5, and 10). The values are also reported in Table 1. At a higher normal location, the average thickness is higher for low Pr numbers and lower for high Pr numbers. For $Pr = 0.1$, the thickness is highest at $y = 10$ and lowest at $y = 2$, showing that heat markers were already carried away from the wall. For $Pr = 100$, the average thickness is highest at $y = 2$ and lowest at $y = 10$. The number of events that were associated with the upwards movement of markers is also shown in Table 1. It can be seen that fewer (and, thus, larger) eddies contribute to heat transfer for low Pr. For example, 13 events contribute to heat transfer for $Pr = 0.1$, indicating a thermal streak spacing of $(2\pi h/13) \approx 73$ wall units at $y = 2$ and an average eddy diameter of 73/2 = 36.5 wall units. For $Pr = 100$, the streak spacing is $(2\pi h/18) \approx 53$ and the associated eddies have a diameter of about 26 wall units.

The picture that emerges now is that, as the Pr increases, a smaller percentage of the eddy cross-section "pumps" heat from the wall to the outer region. The outer edge of the eddies contribute to the transfer of heat at higher Pr. Transport at lower Pr is mostly affected by high molecular diffusion, which results in thicker, more diffuse areas of high heat transport. However, what happens to the heat markers for both low and high Pr when they are already pumped to the outer region? Are the heat markers carried back to the channel wall region by the same eddies that take them away (circulating eddies), or are the heat markers simply just shot up and away from the channel wall by the eddies? This question can be answered by calculating the average normal position as a function of time of the heat markers that are moving away from the wall at time t_1 (i.e., of those markers that are shown in Figs. 3 and 4). This average position is shown in Fig. 6, in comparison with the average normal position of all the particles. For $Pr = 0.1$, the two lines are almost on top of each other. As the Prandtl number increases, the average normal position of the heat particles that were moving away from the wall at time t_1 is rising higher than the average normal position of all the particles. This shows that, on average, the particles that are moving away from the wall at time t_1 will continue to move up into the flow field.

The marker velocities in the y and the z directions were studied for the same subset of heat markers to further verify the findings in Fig. 6 and to identify velocity structures that are related to turbulent heat flux producing structures. The observations are summarized in the schematic of how the eddies carry heat markers away from the wall that is shown in Fig. 7. The physical mechanism of transferring heat away from the wall or towards the wall is associated with couples of counter-rotating eddies one next to the other. The markers are either carried up or moved down by these two eddies. Low Pr fluids, where the molecular diffusivity effects are stronger, can pump heat markers upwards easier utilizing

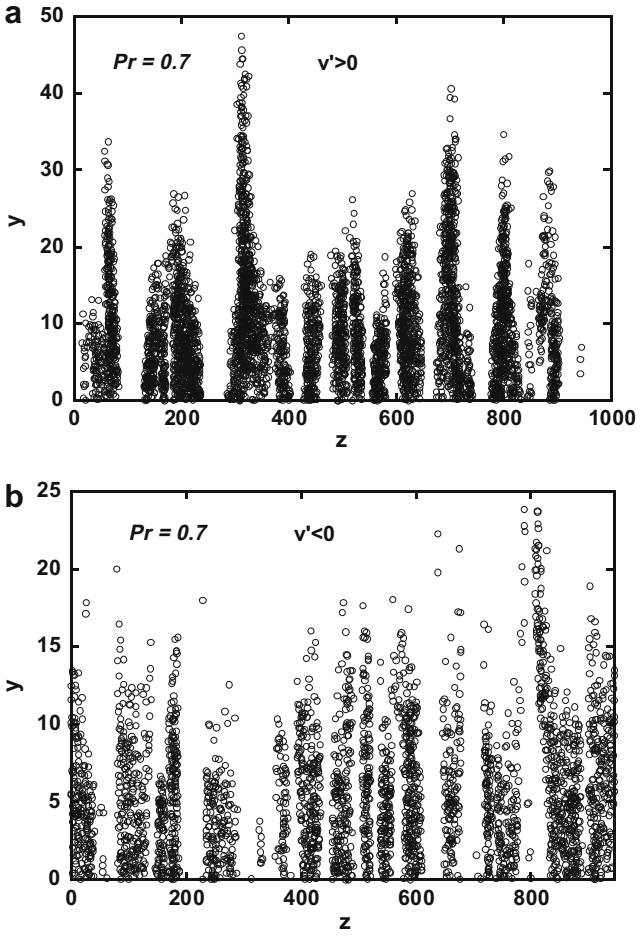

Fig. 3. Positions on the (y, z) plane of markers released from an instantaneous line source in channel flow ($Pr = 0.7$). The downstream location is at $140 < x - x_o < 160$. (a) $v' > 0$, and (b) $v' < 0$.

Table 1
Characteristics of flow structures that move heat markers towards the center of the channel downstream from an instantaneous line source of heat, and number of velocity eddies associated with them. Each of the two runs (A and B) involved the release of 100,000 heat markers at the wall in a turbulent flow channel.

	$Pr = 0.1$	$Pr = 0.7$	$Pr = 6$	$Pr = 10$	$Pr = 100$
Heat markers captured at $140 < x - x_o < 160$					
t_1	31	41	51	61	111
Number of particles – run A	6137	8000	6531	6124	4578
Number of particles – run B	6175	8812	6700	5970	4667
Average thickness of cloud of heat markers moving upwards					
$y = 2$	29.2	31.7	21.3	24.0	22.4
$y = 5$	31.2	35.6	21.1	24.5	6.5
$y = 10$	37.9	36.8	19.4	18.5	0.0
Number of upwards flow events					
Run A					
$y = 2$	13	13	13	12	20
$y = 5$	12	12	15	11	10
$y = 10$	12	12	11	10	0
Run B					
$y = 2$	13	13	18	19	18
$y = 5$	13	10	21	19	12
$y = 10$	11	10	13	10	0

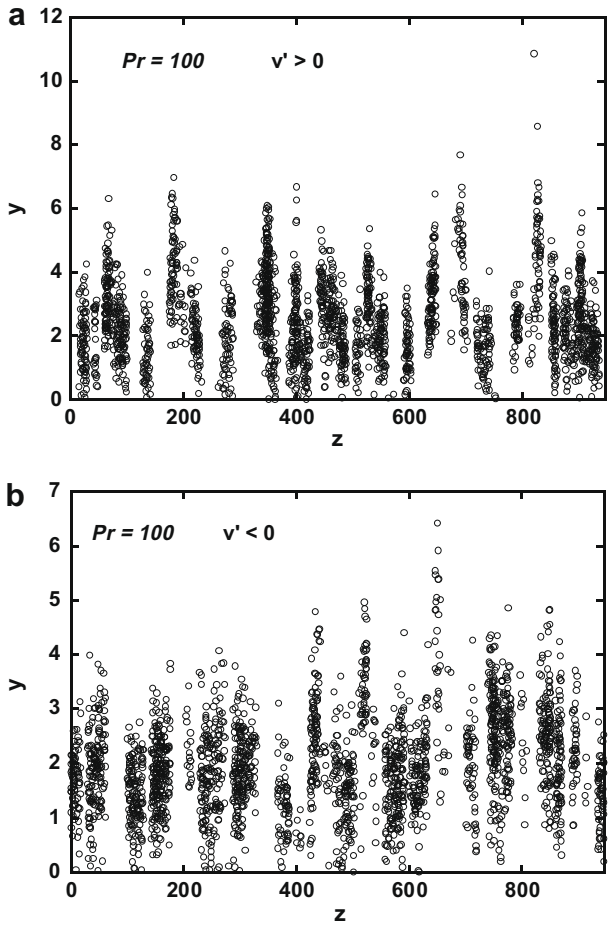

Fig. 4. Positions on the (y, z) plane of markers released from an instantaneous line source in channel flow ($Pr = 100$). The downstream location is at $140 < x - x_o < 160$. (a) $v' > 0$, and (b) $v' < 0$.

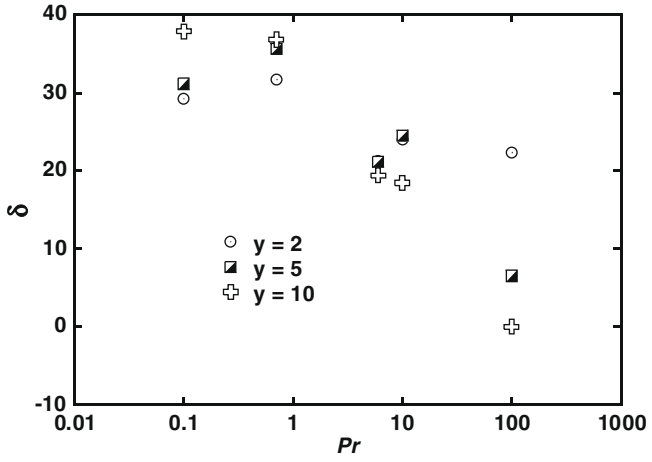

Fig. 5. Average thickness of heat transferring structures downstream from an instantaneous line source at different distances from the wall and for all Prandtl number fluids.

larger eddies for this purpose, and the markers reach out to the outer region. For higher Pr fluids, the thickness of the clouds of particles decreases as shown in Fig. 5, indicating that fewer heat markers are shot upwards. Those markers continue moving upwards, towards the center of the channel, in plumes, as they disassociate from the circular eddies.

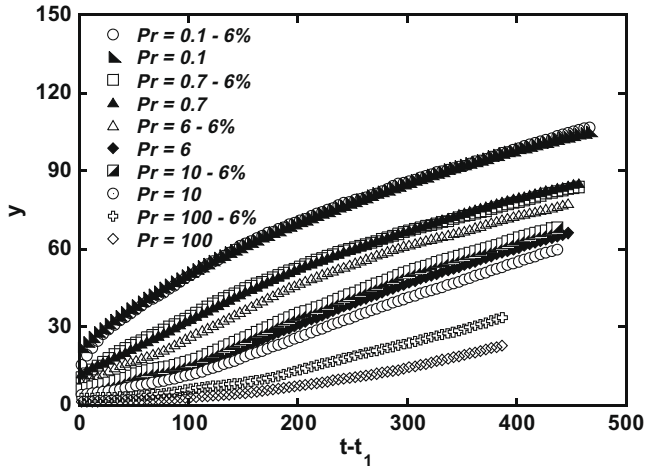

Fig. 6. Average normal position for heat markers that are moving away from the wall.

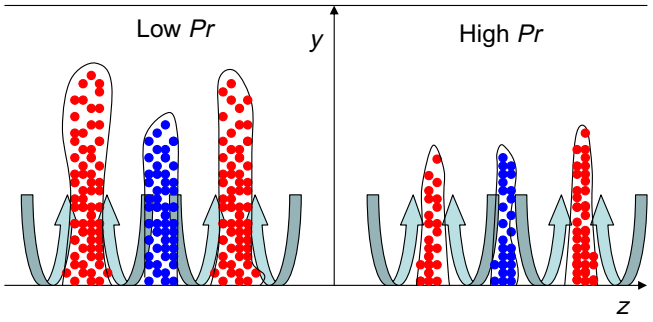

Fig. 7. Schematic of the mechanism of heat transfer away from the wall. For both low and high Pr fluids, heat is transferred from the wall by counter-rotating eddies that pump heat (marked by red particles) towards the outer region of the flow. As the Pr increases, the thickness of the hot areas decreases, as does the height of these areas. Markers pumped upwards continue their upwards trajectories. Transfer of heat towards the wall (marked by blue particles) occurs at the downwards-moving part of these eddies, and it involves markers that have already been in the outer region of the flow.

4.2. The turbulent Prandtl number

A two-point correlation coefficient can be calculated as

$$R_{cc}(y, \Delta z) = \frac{\overline{c'(z_o)c'(z_o + \Delta z)}}{\left(\overline{c'^2(z_o)}\right)^{1/2}\left(\overline{c'^2(z_o)}\right)^{1/2}} \tag{8}$$

The overbar denotes average at a particular y location and $c'(y,z) = C(y,z) - \overline{C}(y)$ as in Eq. (7). The correlation coefficients for plane channel flow and for temperature fields resulting for the heat markers with $v' > 0$ (i.e., for fluctuations such as those shown in Fig. 3) are presented in Fig. 8 for low and high Pr ($Pr = 0.7$ and $Pr = 100$). At the same distance from the wall, the coefficients are smaller as Pr increases. The same correlation coefficient is shown in Fig. 9 for plane Couette flow for $Pr = 0.7$ and 100, respectively. The main difference from plane channel flow is that there is a minimum followed by a maximum that indicates a very strong correlation between the structures that transfer heat. For low Pr, the correlation coefficients are approximately the same at all distances. For high Pr, the values of the correlation coefficient are smaller closer to the wall.

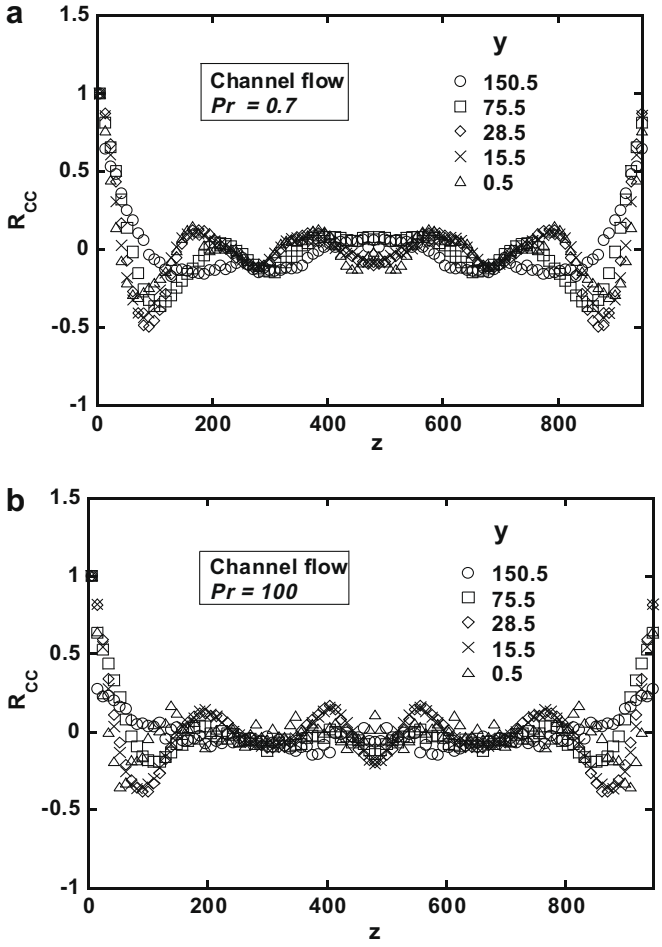

Fig. 8. Correlation coefficient in the spanwise direction for heat transferring structures away from the wall in channel flow: (a) $Pr = 0.7$, and (b) $Pr = 100$.

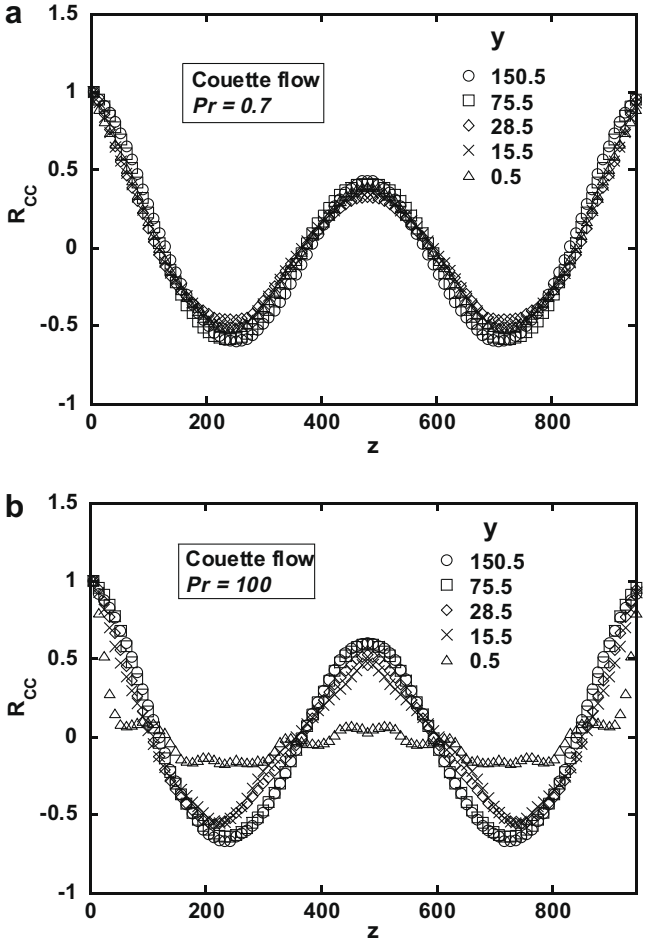

Fig. 9. Correlation coefficients in the spanwise direction for heat transferring structures away from the wall in Couette flow: (a) $Pr = 0.7$, and (b) $Pr = 100$.

Fig. 10(a and b) present the length scale that is obtained by the correlation coefficient as a function of normal distance, which can be calculated as

$$L_T = \int_{z_o}^{\infty} R_{cc}(z)dZ \tag{9}$$

for plane channel and plane Couette flow, respectively. The physical meaning of these length scales is that they characterize the structures that produce turbulent heat flux. These are the length scales that would indicate the thickness of thermal streaks in the case of Eulerian analysis of turbulent heat transfer from the wall. The length scales are larger in plane Couette flow. In both cases, the length scales are higher in the outer region. In plane channel flow, the length scales increase as y increases. The length scales do not show a distinctive dependence on Prandtl numbers. In plane Couette flow, the length scale shows dependence on Pr closer to the wall.

Following the analysis of Crimaldi et al. [22], the turbulent Prandtl number was calculated as

$$Pr_\tau \equiv \frac{L_M}{L_T} \tag{10}$$

where L_M is the length scale for the fluid particles and L_T is the length scale for the heat markers, both of which were calculated as in Eq. (9). Note that Eq. (10) is not the ratio of the mixing lengths, as in the work of Crimaldi et al., but is the ratio of the length scales obtained with a Lagrangian analysis, which are assumed to be proportional to the mixing lengths. Furthermore, the ratio of the proportionality constants is assumed to be on the order of one, so that Eq. (10) can yield the turbulent Prandtl number.

The turbulent Prandtl number for plane channel and plane Couette flows as a function of the distance from the wall is shown in Fig. 11(a and b), respectively. A statistic Q-test [41] with sample size of 6 was conducted in order to remove any outlier points at 90% confidence interval. The error bars have a width equal to two standard deviations calculated based on the data of the different simulation runs excluding the outlier points. As presented in these figures, the average Pr_τ for all cases falls within the error bars. Based on these results, it can be concluded that there is no statistically significant dependence of Pr_τ on Pr. There is, however, dependence on the distance from the wall.

Turbulent Prandtl numbers for fluids with $Pr = 0.1$, 0.7 and 6 are compared with previous DNS data by Kawamura et al. [13,14] and by Kasagi's group [15] in Fig. 12. The results obtained herein agree with these previous DNS data. Finding the turbulent Prandtl number using the length scales obtained through a Lagrangian analysis has not been accomplished before, but it shows reasonable results compared to other methods.

5. Conclusions

The correlation between the structure of the velocity field and the thermal field has been investigated and visualized. The velocity field has a strong impact on the thermal field. The mechanism of heat transfer away from the wall was studied using markers of

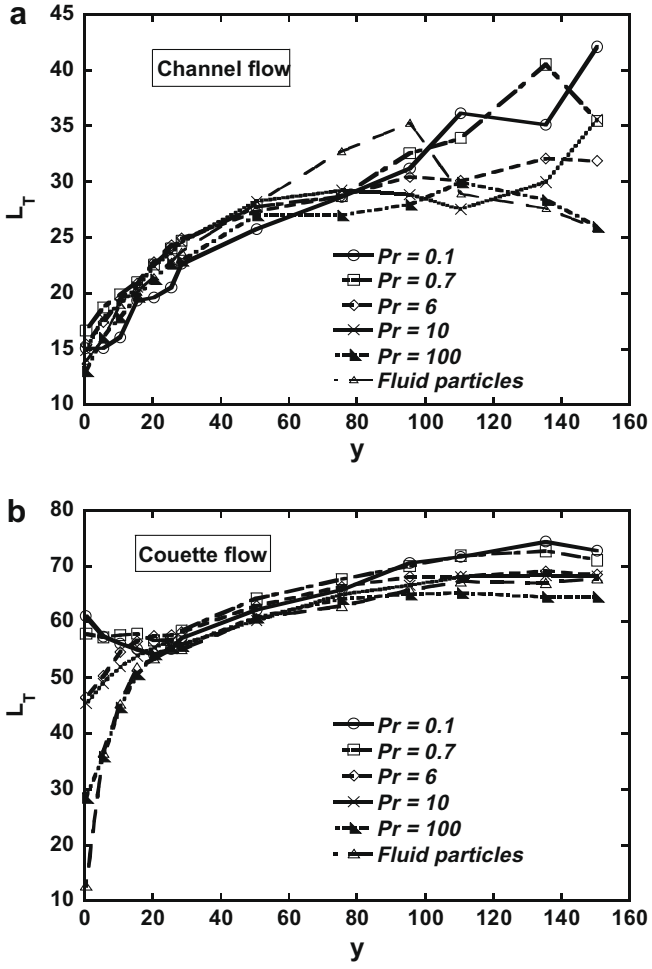

Fig. 10. Length scales characteristic of heat transfer for: (a) channel flow, and (b) Couette flow.

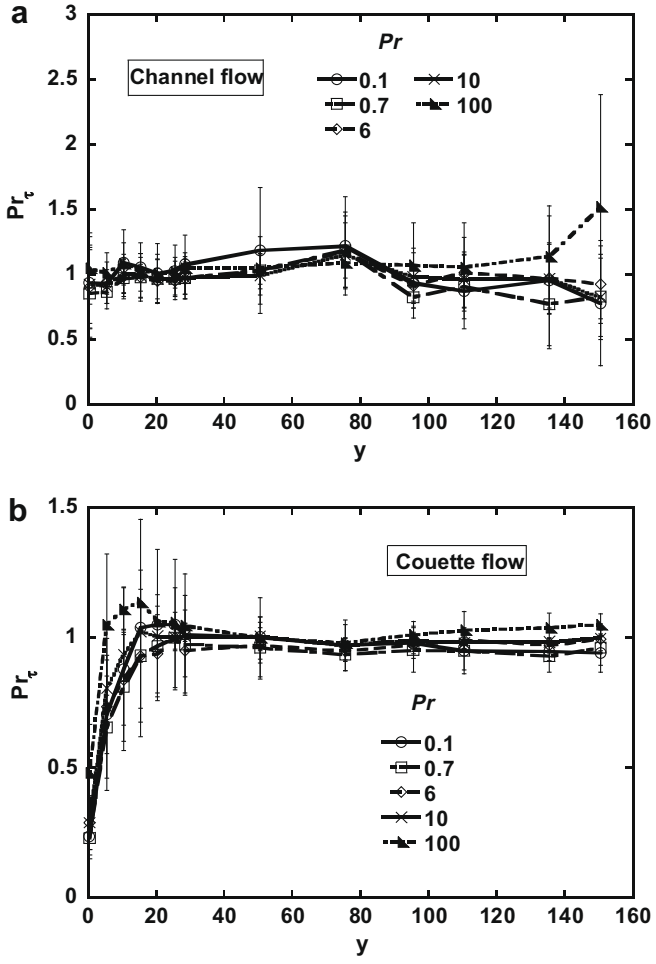

Fig. 11. Turbulent Prandtl number as a function of the fluid Prandtl number and the distance from the wall for: (a) channel flow, and (b) Couette flow.

heat emitted from single line sources. The presence of these markers at high concentration in specific locations in the flow field marked the location of hot or cold areas. Couples of counter-rotating eddies carry heat particles away or towards the wall. The markers that move away tend to continue their upwards trajectories towards the center of the channel and are not carried back down by the same eddies. For lower Prandtl numbers, the thickness of the marker clouds are larger and the particles shoot up further into the outer region, indicating that the thickness of the turbulent heat flux producing thermal streaks is larger for lower *Pr*.

The turbulent Prandtl numbers were calculated by the ratio of the length scales of fluid particles to the length scale of heat markers at specific *Pr*. The results showed a good agreement with previously reported DNS data. However, this Lagrangian methodology of obtaining the turbulent Prandtl number shows that it has no statistically significant dependence on the fluid Prandtl number, but it has a dependence on the distance from the wall.

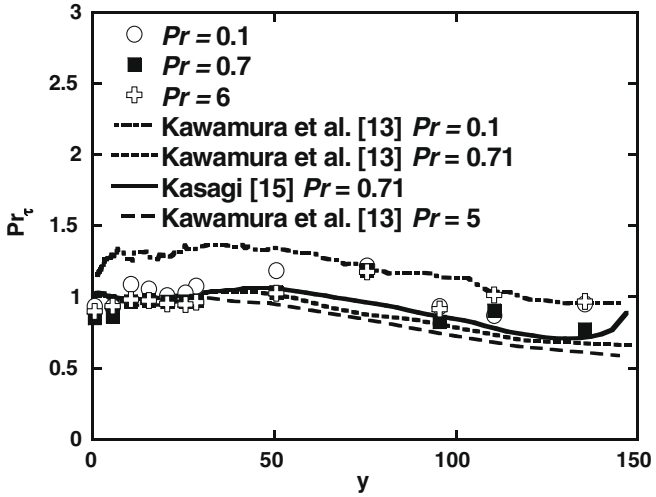

Fig. 12. Comparison with other reported turbulent Prandtl numbers.

Acknowledgements

The support of NSF under CBET-0651180 is gratefully acknowledged. This work was also supported by the National Computational Science Alliance under CTS040023 and the TeraGrid under CT070050, and utilized the NCSA IBMp690, and the SDSC Datastar IBMp690. Computational support was also offered by the University of Oklahoma Center for Supercomputing Education and Research (OSCER).

References

[1] S.K. Robinson, Coherent motions in the turbulent boundary layer, Annu. Rev. Fluid Mech. 23 (1991) 601–639.
[2] Y. Nagano, M. Tagawa, Coherent motions and heat transfer in a wall turbulent shear flow, J. Fluid Mech. 306 (1995) 127–157.

[3] R. Nagaosa, Direct numerical simulation of vortex structures and turbulent scalar transfer across a free surface in a fully developed turbulence, Phys. Fluids 11 (6) (1999) 1581–1595.
[4] J. Jeong, F. Hussain, W. Schoppa, J. Kim, Coherent structures near the wall in a turbulent channel flow, J. Fluid Mech. 332 (1997) 185–214.
[5] T.J. Hanratty, D.V. Papavassiliou, The role of wall vortices in producing turbulence, in: R.L. Panton (Ed.), Self Sustaining Mechanisms of Wall Turbulence, Computational Mechanics, Inc., 1997, pp. 83–108.
[6] R.A. Handler, J.R. Saylor, R.I. Leighton, A.L. Rovelstad, Transport of a passive scalar at a shear-free boundary in a fully developed turbulent open channel flow, Phys. Fluids 11 (9) (1999) 2607–2625.
[7] I. Marusic, On the role of large-scales structures in wall turbulence, Phys. Fluids 13 (3) (2001) 736–743.
[8] H. Abe, H. Kawamura, Y. Matsuo, Direct numerical simulation of a fully developed turbulent channel flow with respect to the Reynolds number dependence, J. Fluid Eng. – Trans. ASME 123 (2) (2001) 382–393.
[9] B. Ganapathisubramani, E.K. Longmire, I. Marusic, Experimental investigation of vortex properties in a turbulent boundary layer, Phys. Fluids 18 (5) (2006) 055105.
[10] V.K. Natrajan, K.T. Christensen, The role of coherent structures in subgrid-scale energy transfer within the log layer of wall turbulence, Phys. Fluids 18 (6) (2006) 065104.
[11] R. Camussi, F.D. Felice, Statistical properties of vertical structures with spanwise vorticity in pressure gradient turbulent boundary layers, Phys. Fluids 18 (3) (2006) 035108.
[12] N. Hutchins, I. Marusic, Large-scale influences in near-wall turbulence, Philos. Trans. R. Soc. A 365 (2007) 647–664.
[13] H. Kawamura, H. Abe, Y. Matsuo, DNS of turbulent heat transfer in channel flow with respect to Reynolds and Prandtl number effects, Int. J. Heat Fluid Flow 20 (1999) 196–207.
[14] H. Abe, H. Kawamura, Y. Matsuo, Surface heat-flux fluctuations in a turbulent channel flow up to Re-tau = 1020 with Pr = 0.025 and 0.71, Int. J. Heat Fluid Flow 25 (3) (2004) 404–419.
[15] N. Kasagi, Y. Ohtsubo (1992). Available from: <http://www.thtlab.t.u-tokyo.ac.jp/>.
[16] D.V. Papavassiliou, Turbulent transport from continuous sources at the wall of a channel, Int. J. Heat Mass Transfer 45 (17) (2002) 3571–3583.
[17] D.V. Papavassiliou, Scalar dispersion from an instantaneous source at the wall of a turbulent channel for medium and high Prandtl fluids, Int. J. Heat Fluid Flow 23 (2) (2002) 161–172.
[18] B.M. Mitrovic, D.V. Papavassiliou, Transport properties for turbulent dispersion from wall sources, AIChE J. 49 (5) (2003) 1095–1108.
[19] B.M. Mitrovic, P.M. Le, D.V. Papavassiliou, On the Prandtl or Schmidt number dependence of the turbulence heat or mass transfer coefficient, Chem. Eng. Sci. 59 (3) (2004) 543–555.
[20] P.M. Le, D.V. Papavassiliou, Turbulent heat transfer in plane Couette flow, J. Heat Transfer – Trans. ASME 128 (1) (2006) 53–62.
[21] P.M. Le, D.V. Papavassiliou, Turbulent dispersion from elevated line sources in plane channel and plane Couette flow, AIChE J. 51 (9) (2005) 2402–2414.
[22] J.P. Crimaldi, J.R. Koseff, S.G. Monismith, A mixing-length formulation for the turbulent Prandtl number in wall-bounded flows with bed roughness and elevated scalar sources, Phys. Fluids 18 (9) (2006) 095102.
[23] S.W. Churchill, Progress in the thermal sciences: AICHE Institute Lecture, AIChE J. 46 (9) (2000) 1704–1722.
[24] A.J. Reynolds, Prediction of turbulent Prandtl and Schmidt numbers, Int. J. Heat Mass Transfer 18 (1975) 1055–1069.
[25] D. Hollingsworth, W. Kays, R. Moffat, Measurements and prediction of the turbulent thermal boundary layer in water on flat and concave surfaces, Technical Report HMT-41, Thermosciences Division, Department of Mechanical Engineering, Stanford University, Stanford, CA, 1989.
[26] A. Snijders, A. Koppius, C. Nieuwvelt, D. deVries, An experimental determination of the turbulent Prandtl number in the inner boundary layer for an air flow over a flat plate, in: Sixth International Heat Transfer Conference, vol. 2, Toronto, Canada, 1978, pp. 519–523.
[27] W.M. Kays, Turbulent Prandtl number – where are we?, J Heat Transfer – Trans. ASME 116 (2) (1994) 284–295.
[28] S.W. Churchill, C. Chan, Turbulent flow in channels in terms of the turbulent shear and normal stresses, AIChE J. 41 (12) (1995) 2513–2521.
[29] D.V. Papavassiliou, T.J. Hanratty, Transport of a passive scalar in a turbulent channel flow, Int. J. Heat Mass Transfer 40 (6) (1997) 1303–1311.
[30] Y. Mito, T.J. Hanratty, Lagrangian stochastic simulation of turbulent dispersion of heat markers in a channel flow, Int. J. Heat Mass Transfer 46 (6) (2003) 1063–1073.
[31] D.V. Papavassiliou, T.J. Hanratty, The use of Lagrangian methods to describe turbulent transport of heat from the wall, Ind. Eng. Chem. Res. 34 (10) (1995) 3359–3367.
[32] K. Kontomaris, T.J. Hanratty, J.B. McLaughlin, An algorithm for tracking fluid particles in a spectral simulation of turbulent channel flow, J. Comput. Phys. 103 (1993) 231–242.
[33] N. Kasagi, Y. Tomita, A. Kuroda, Direct numerical simulation of passive scalar field in a turbulent channel flow, J. Heat Transfer – Trans. ASME 114 (3) (1992) 598–606.
[34] S.L. Lyons, T.J. Hanratty, J.B. McLaughlin, Large-scale computer-simulation of fully-developed turbulent channel flow with heat-transfer, Int. J. Numer. Meth. Fluids 13 (8) (1991) 999–1028.
[35] C. Liu, Turbulent plane Couette flow and scalar transport at low Reynolds number, J. Heat Transfer – Trans. ASME 125 (2003) 988–998.
[36] D. Lakehal, M. Fulgosi, S. Banerjee, G. Yadigaroglu, Turbulence and heat exchange in condensing vapor–liquid flow, Phys. Fluids 20 (2008) 065101.
[37] F. Schwertfirm, M. Manhart, DNS of passive scalar transport in turbulent channel flow at high Schmidt numbers, Int. J. Heat Fluid Flow 28 (6) (2007) 1204–1214.
[38] A. Gunther, D.V. Papavassiliou, M.D. Warholic, T.J. Hanratty, Turbulent flow in channel at low Reynolds number, Exp. Fluids 25 (5–6) (1998) 503–511.
[39] D.V. Papavassiliou, T.J. Hanratty, Interpretation of large scale structures in a turbulent plane Couette flow, Int. J. Heat Fluid Flow 18 (1) (1997) 55–69.
[40] P.G. Saffman, On the effect of the molecular diffusivity in turbulent diffusion, J. Fluid Mech. 8 (1960) 273–283.
[41] R.B. Dean, W.J. Dixon, Simplified statistics for small numbers of observations, Anal. Chem. 23 (4) (1951) 636–638.